Energy Transfer between Polyatomic Molecules II: Energy Transfer Quantities and Probability Density Functions in Benzene, Toluene, *p*-Xylene, and Azulene Collisions†

V. Bernshtein and I. Oref*

Department of Chemistry, Technion-Israel institute of Technology, Haifa 32000, Israel

Received: June 30, 2005; In Final Form: September 18, 2005

Collisional energy transfer, CET, is of major importance in chemical, photochemical, and photophysical processes in the gas phase. In Paper I of this series (*J. Phys. Chem. B* **2005**, *109*, 8310) we have reported on the mechanism and quantities of CET between an excited benzene and cold benzene and Ar bath. In the present work, we report on CET between excited toluene, *p*-xylene, and azulene with cold benzene and Ar and on CET of excited benzene with cold toluene, *p*-xylene, and azulene. We compare our results with those of Paper I and report average vibrational, rotational, and translational energy quantities, $\langle \Delta E \rangle$, transferred in a single collision. We discuss the effect of internal rotation on CET and the identity of the gateway modes in CET and the relative role of vibrational, rotational, and translational energies in the CET process, all that as a function of temperature and excitation energy. Energy transfer probability density functions, $P(E,E')$, for the various systems are reported and the shape of the curves for various systems and initial conditions is discussed. The major findings for polyatomic−polyatomic collisions are: CET takes place mainly via vibration-to-vibration energy transfer assisted by overall rotations. Internal free rotors in the excited molecule hinder energy exchange while in the bath molecule they do not. Energy transfer at low temperatures and high temperatures is more efficient than that at intermediate temperatures. Low-frequency modes are the gateway modes for energy transfer. Vibrational temperatures affect energy transfer. The CET probability density function, $P(E,E')$, is convex at low temperatures and can be concave at high temperatures. A mechanism that explains the high values of $\langle \Delta E \rangle_a$ and the convex shape of $P(E,E')$ is that in addition to short impulsive collisions there are chattering collisions where energy is transferred in a sequence of short encounters during the lifetime of the collision complex. This also leads to the observed supercollision tail at the down wing of $P(E,E')$. Polyatomic−Ar collisions show mechanistic similarities to polyatomic−polyatomic collisions, but there are also many dissimilarities: internal rotations do not inhibit energy transfer, $P(E,E')$ is concave at all temperatures, and there is no contribution of chattering collisions.

Introduction

Collisional energy transfer, CET, plays a major role in chemical, photochemical, and photophysical processes.[1] Activation and deactivation of molecules are the vehicles through which energy is pumped in and out of molecules, enabling them to undergo chemical transformations. However, the detailed mechanism of CET in large polyatomic−polyatomic, PP, collisions is not well known. In addition, the experimental results of large PP CET explored by IR fluorescence, UV absorption, and kinetically controlled selective ionization lack in consistency.[2] The deficiency in the understanding of PP CET in the gas phase is the motivation for embarking on a systematic and comprehensive study of these systems. The present article is the second in a series of articles that discuss energy transfer in collisions between polyatomic molecules in the gas phase. The first article in the series,[3] paper I, dealt with collisions between excited benzene, B*, and cold benzene bath, B, and the results were compared to B−Ar collisions. The third article will deal with CET in self-collisions. The major findings in paper I are the following: The mechanism of energy transfer in PP collisions differs in principle from that of polyatomic−monatomic, PM, collisions. The major channel for energy transfer in PP collisions is vibration-to-vibration, V−V, energy transfer, assisted by rotations, whereas in PM it is vibration/rotation-to-translation, V−R−T, energy transfer. Large values of ΔE and supercollisions can occur in PP by multiple encounters during the lifetime of the collision complex, whereas in PM supercollisions occur when the incoming atom is in phase with an out-of-plane, OOP, vibration and overall rotations.[4−6] The shape of the down-collisions wing of the probability density function $P(E,E')$ in PP collisions is convex at low temperatures and becomes a straight line or even slightly concave at higher temperatures. The shape of the down-collisions wing of $P(E,E')$ in PM collisions is concave at moderate and high temperatures with a noticeable supercollision tail. The $P(E,E')$ are represented as semilog plots in order to accommodate the few orders of magnitude in the probability function. The value of total average energy transferred per collision, $\langle \Delta E \rangle_a$, in PP collisions is much larger than that in a PM collision because of the fact that there is an extra V−V channel that is absent in the latter. The V−R channel is similar in both systems. The collision complex lifetime has no effect on the value of ΔE in PM collisions because the actual CET event occurs in the last few tenths of femtoseconds of the collision complex lifetime.[7] How long the atom hovers over the polyatomic molecule has no effect on the

† Part of the special issue "William Hase Festschrift".

* Corresponding author. E-mail: chroref@technion.ac.il.

10.1021/jp053582l CCC: $33.50
Published on Web 10/20/2005

final outcome. In PP collisions, however, collision lifetimes do affect the values of ΔE inasmuch as multiple encounters occur during the collision lifetime, each transferring a given amount of vibrational energy to the cold polyatomic bath. Freezing rotations enhance CET in PP because they enable the formation of a collision complex and hinder it in PM because the rotation-to-translation channel is blocked.

Paper I also discusses the common features of PP and PM collisions; identical and very small net overall rotational energy, $\langle\Delta E_R\rangle_a$, is transferred during the CET but the average values of the up and down CET, $\langle\Delta E_R\rangle_{u,d}$, are large, which indicate active participation of rotations in the energy transfer process. Also common are the existence of gateway modes in CET. In both cases they proved to be the low-frequency OOP modes of the excited polyatomic molecule. Overall, translational energy transfer values, $\langle\Delta E_T\rangle_a$, in PP and PM collisions are small and almost identical. However, the values of the average up and down transfer,$\langle\Delta E_T\rangle_{u,d}$, are fairly large, between 100 and 250 cm^{-1} depending on the temperature, but because there are equal chances for both up and down events, the net $\langle\Delta E_T\rangle_a$ is small. Despite its importance to CET, translational energy transfer contributes only a fraction to the overall energy transfer in PP collisions, V−V, being the major channel, it is the only CET channel in PM collisions, which explains their small $\langle\Delta E\rangle_a$ values.

An extensive list of references dealing with previous experimental and computational work on CET is listed in paper I, and readers interested in general background can find it there. In the present work we expend our previous work by studying collisions of excited toluene, T*, *p*-xylene, pX*, and azulene, AZ*, with cold benzene, B, bath, and B* collisions with T, pX, and AZ bath and compare the results with B*-B CET reported in Paper I. The present work also presents results and discusses collisions between T*, pX*, AZ*, and Ar, and a comparison is made between polyatomic and monatomic colliders. We explore the effect of internal rotation on CET by comparing T and pX to B and AZ. It should be pointed out that pX and AZ are structurally different but have the same number of normal modes and hence very similar vibrational−rotational temperatures, which should facilitate a comparison between the CET quantities of the two molecules. In another part of this work, we assign identical vibrational−rotational temperatures to all four molecules and study the individual CET quantities under these conditions.

Theory

The numerical methods used in the present work are reported in Paper I and in refs 7 and 8. The classical equations of motion that describe the relative motion of the colliding pair include the inter- and intramolecular potentials. The intramolecular potential includes all of the normal mode contributions, stretching, bending, torsion, and wagging. The values of the parameters of this potential for B, T, and pX were obtained from valence force field calculations by Draeger[9] and were modified slightly to give the best agreement of calculated to experimental normal-mode frequencies, especially the low-frequency ones. The experimental and calculated frequencies are given in Appendix IV. The force constants for AZ were taken from Lim and Gilbert[10] and modified to reproduce the experimental normal modes frequencies. The parameters of the pairwise intermolecular Lennard−Jones (LJ) potential of B−B, which are reported in Paper I, were used for the rest of the aromatic molecules in the series. This way, a consistent set of PP potentials was obtained. This enabled a comparison between CET quantities obtained for various colliders and excited molecules. The goodness of the parameters was checked by using the pairwise collision radius, σ_{ij}, and well depth, ϵ_{ij}, for C−C, C−H, and H−H interaction and calculating the literature value for the effective LJ σ and ϵ for each molecule in a manner suggested by Lim[11] and used by the program SIGMON.[12] Good agreement with experimental values was obtained. A table of experimental and calculated values of σ and ϵ together with pairwise parameters σ_{ij} and ϵ_{ij} are presented in Appendix I (see the footnote in the Appendix). The LJ pairwise parameters for the Ar−polyatomic collisions were based on the B−Ar values calculated by SIGMON[12] but adjusted slightly to give best fit to σ and ϵ obtained from the literature. The parameters used in the calculations are given in Appendix II. To further check the reliability of the intermolecular parameters, we have compared the ϵ and σ for B−Ar obtained from LJ pairwise potential with those obtained from ab initio calculations by Bludsky, Spirko, Herouda, and Hobza (BSHH).[13] The results are in good agreement: $\sigma_{LJ} = 0.447$ nm, $\epsilon_{LJ}/k = 214$ K, $\sigma_{BSSH} = 0.436$ nm, and $\epsilon_{BSSH}/k = 309$ K. The full details are given in Appendix II.

The equations of motion were integrated by using a modified computer program, Venus.[14] The initial relative translational and rotational energies were chosen from the appropriate thermal distributions. The initial impact parameter was chosen randomly from values between 0 and its maximum value, b_m. The value of the maximum impact parameter was determined separately for each molecule.[7,8] The values of b_m were: b_m(B*−B) = 1.3 nm; b_m(B*−T) = 1.2 nm; b_m(T*−B) = 1.2 nm; b_m(pX*−B) = 1.35 nm; b_m(AZ*−B) = 1.3 nm; The initial vibrational energy was assigned in two ways. In one, constant photon energy of 40 700 cm^{-1} was assigned to all molecules and the thermal energy at each temperature was added to it. In the second, the vibrational temperature, T_V, of all molecules was assigned the T_V of excited benzene plus thermal energy and was kept constant for the whole series. For constant excitation energy, the average energy per mode in molecules of different sizes will be different. This might affect the values of the various $\langle\Delta E\rangle$ quantities. A unifying physical property is the vibrational temperature. After a molecule absorbs a photon, fast internal conversion occurs[15] and the ergodic molecule can be assumed to have a vibrational temperature given by:

$$E + \sum_i h\nu_i/[\exp(h\nu_i/kT) - 1] = \sum_i h\nu_i/[\exp(h\nu_i/kT_V) - 1] \quad (1)$$

In the present calculations, E is the excitation energy of benzene (40 700 cm^{-1}). The second term is the thermal energy where ν_i is the frequency of the ith normal mode and T is the ambient temperature. The vibrational temperature, T_V, was found by iteration. Once T_V for B was found, it was substituted in eq 1 and the internal energy of each of the molecules was calculated. Of the four molecules studied, three have a different number of normal modes, and therefore T_V is a unifying feature. A table of vibrational temperatures and internal energies for all four molecules at the temperatures studied is given in Appendix III.

The collision duration was determined by monitoring the beginning and end of each collision by the forward and backward sensing (FOBS) method.[7,8,16] In the FOBS method, a collision is defined by a change, ϵ, in the internal energy of the excited molecule in a time interval, Δt. After careful and exhaustive study, the ratio $\epsilon/\Delta t$ was taken to be 0.35 cm^{-1}/fs. Approximately 50 000 trajectories were used for each set of

TABLE 1: Energy Transfer Quantities of the Excited Molecule in Polyatomic−Polyatomic Collisions[a]

	excited molecule				cold molecule			
	B*−B	T*−B	pX*−B	AZ*−B	B*−B	T*−B	pX*−B	AZ*−B
$\langle\Delta E\rangle_a$	−755	−643	−551	−765	737	614	529	694
$\langle\Delta E\rangle_d$	−888	−766	−690	−888	−53	−65	−69	−61
$\langle\Delta E\rangle_u$	55	73	91	77	869	728	651	805
$\langle\Delta E_V\rangle_a$	−767	−657	−558	−784	731	600	515	636
$\langle\Delta E_V\rangle_d$	−874	−766	−678	−894	−13	−15	−21	−20
$\langle\Delta E_V\rangle_u$	27	55	62	61	815	674	593	709
$\langle\Delta E_R\rangle_a$	12	14	8	19	7	14	14	58
$\langle\Delta E_R\rangle_d$	−126	−114	−116	−120	−126	−135	−130	−131
$\langle\Delta E_R\rangle_u$	144	132	124	141	136	147	146	204
$\langle\Delta E^{H+C_T}\rangle_a$	18	30	21	71				
$\langle\Delta E^{H+C_T}\rangle_d$	−136	−150	−151	−147				
$\langle\Delta E^{H+C_T}\rangle_u$	157	182	182	235				
$\langle\tau_{coll}\rangle_a$	2.23	2.28	2.54	2.51	2.23	2.28	2.54	2.51
$\langle\tau_{coll}\rangle_d$	2.39	2.44	2.75	2.66	1.27	1.36	1.46	1.44
$\langle\tau_{coll}\rangle_u$	1.29	1.39	1.56	1.47	2.39	2.44	2.76	2.66

[a] $E_v = 40\,700$ cm^{-1} plus thermal energy at 300 K. The units of $\langle\Delta E\rangle$ are in cm^{-1} and the units of $\langle\tau_{coll}\rangle$ are in ps. $\langle\Delta E^{H+C_T}\rangle$ indicates the total translational energy gained or lost by the hot and cold molecules

initial conditions. A large number of trajectories were used in order to provide good statistical sampling in the binning process. The FOBS method was also used in identifying effective collisions among the total elastic and inelastic collisions.

The average energy transferred quantities were calculated by the following equation

$$\langle\Delta E_X\rangle_Y = \sum_i^{N_j} \Delta E_X/N_j \tag{2}$$

Where X can be V, R, or T. ΔE without X indicate "all" quantities. Y indicates up, down, or all quantities. N_j indicates the number of effective trajectories as determined by FOBS. For example, in $\langle\Delta E_V\rangle_d$ the effective N_j is the number of all trajectories in which the molecule lost vibrational energy. The value of N_j changes for each quantity; therefore, N_j for $\langle\Delta E_V\rangle_d$ is different than that for $\langle\Delta E_T\rangle_d$. However, when we compare our results to the experimental ones, we always use the total number of collisions, effective or not. The disadvantage of using the total number of trajectories instead of effective ones when studying the mechanism of CET is that a good number of them describe large-impact parameter elastic collisions that do not transfer energy at all. By mixing elastic and inelastic collisions, we get average CET quantities that are smaller than the actual average energy transferred in a collision. Therefore, we report results for both effective and total number of trajectories. We use the former to draw mechanistic conclusions and the latter for comparison with experimental results and other computational work reported in the literature.

In comparing the present results with experiments, we have used the following expression

$$\langle\Delta E\rangle = \langle\Delta E\rangle_{trj}\frac{b_m^2}{b_{ref}^2} \tag{3}$$

where $b_{ref} = (\sigma_{LJ}^2\Omega^{(2,2)*})^{1/2}$and $\langle\Delta E\rangle_{trj} = (\sum_{i=1}^{N_{trj}}\Delta E_i)/N_{trj}$, b_m is the maximum impact parameter, $\Omega^{(2,2)*}$ is the collision integral, and N_{trj} is the total number of trajectories.

Below we report on collisional energy transfer between excited toluene, *p*-xylene, and azulene with cold benzene bath and excited benzene collisions with toluene, *p*-xylene, and azulene. We also report and discuss collisions between excited toluene, *p*-xylene, azulene, and Ar bath, and a comparison is made between polyatomic and monatomic colliders.

Results and Discussion

The results of the computations of CET enable us to gain insight into the mechanism of CET between polyatomic molecules. The details are given below.

Energy Transfer Quantities at Constant Internal Excitation. In this part, we report on CET of the four molecules excited at a fixed internal energy of 40 700 cm^{-1}. The thermal energy at the ambient temperature was added to this value. Here, only effective trajectories that lead to collisions, as defined by FOBS, are considered. From effective trajectories, it is possible to find the actual amount of energy that is transferred per collision and the detailed mechanism of energy transfer. In addition, bulk $\langle\Delta E\rangle$ will be compared to the experimental results.

The results of CET of collisions of B*, T*, pX*, and AZ* with B as a bath at 300 K are given in Table 1. A clear trend is seen in the values of $\langle\Delta E\rangle$ for all and down collisions. The absolute values decrease in the following order $\langle\Delta E\rangle_{AZ} \approx \langle\Delta E\rangle_B > \langle\Delta E\rangle_T > \langle\Delta E\rangle_{pX}$. As can be seen, pX*, with two internal rotors, transfers on the average less than T* with one rotor. However, CET in AZ*, with the same number of internal modes as pX* but without internal rotors, is much more efficient than pX*. Internal free rotors in the bath gas, however, do not inhibit CET, as is evident from a comparison of the results in Table 1 with those in Table 2. The values of $\langle\Delta E\rangle$ in B* collisions with T, pX, and AZ as a bath gas are larger than those in excited polyatomic−benzene collisions. That is to say, internal free rotors in the cold bath molecules do not inhibit CET, whereas in the excited molecule they inhibit CET. Az is more efficient than B as a bath. Both do not have internal rotations, but B is missing the large number of low-lying modes that are available in AZ. A graphical presentation of the results is given in Figure 1. It shows that the same general behavior is true over a wide temperature range.

To understand the mechanism of the CET process, we have monitored, simultaneously with energy loss in the excited molecule, the energy gain in the cold bath molecule with only thermal energy. The results are also given in Table 1, which shows the energy gain and loss in the hot and cold molecule subsets of trajectories. As can be seen, CET is mainly through

TABLE 2: Energy Transfer Quantities of Excited Benzene Colliding with Bath Toluene, *p*-Xylene, and Azulene[a]

	excited molecule				cold molecule			
$T = 300$ K	B*−B	B*−T	B*−pX	B*−AZ	B*−B	B*−T	B*−pX	B*−AZ
$\langle\Delta E\rangle_a$	−755	−735	−855	−864	737	729	857	861
$\langle\Delta E\rangle_d$	−889	−864	−992	−1000	−53	−49	−47	−58
$\langle\Delta E\rangle_u$	55	45	40	42	869	856	989	998
$\langle\Delta E_V\rangle_a$	−767	−744	−851	−863	731	733	861	864
$\langle\Delta E_V\rangle_d$	−874	−842	−965	−971	−13	−34	−21	−41
$\langle\Delta E_V\rangle_u$	27	37	30	28	815	836	958	986
$\langle\Delta E_R\rangle_a$	12	9	−4	0	7	−4	−4	−3
$\langle\Delta E_R\rangle_d$	−126	−132	−131	−132	−126	−116	−114	−118
$\langle\Delta E_R\rangle_u$	144	140	131	132	136	112	111	113
$\langle\Delta E^{H+C_T}\rangle_a$	18	7	−3	2				
$\langle\Delta E^{H+C_T}\rangle_d$	−136	−146	−152	−154				
$\langle\Delta E^{H+C_T}\rangle_u$	157	154	153	156				
$\langle\tau_{coll}\rangle_a$	2.23	2.57	2.92	3.17	2.23	2.57	2.92	3.17
$\langle\tau_{coll}\rangle_d$	2.39	2.77	3.15	3.41	1.27	1.37	1.36	1.58
$\langle\tau_{coll}\rangle_u$	1.29	1.36	1.41	1.59	2.39	2.77	3.15	3.41
	excited molecule				cold molecule			
$T = 60$ K	B*−B	B*−T	B*−pX	B*−AZ	B*−B	B*−T	B*−pX	B*−AZ
$\langle\Delta E\rangle_a$	−775	−787	−802	−796	756	776	825	806
$\langle\Delta E\rangle_d$	−1027	−1020	−1031	−1043	−115	−88	−89	−115
$\langle\Delta E\rangle_u$	106	81	87	98	1012	1001	1048	1060
$\langle\Delta E_V\rangle_a$	−781	−789	−784	−781	754	795	846	818
$\langle\Delta E_V\rangle_d$	−1005	−976	−970	−989	−44	−69	−53	−86
$\langle\Delta E_V\rangle_u$	71	54	64	75	963	979	1031	1038
$\langle\Delta E_R\rangle_a$	6	2	−19	−15	1	−19	−21	−12
$\langle\Delta E_R\rangle_d$	−212	−220	−226	−230	−219	−193	−190	−194
$\langle\Delta E_R\rangle_u$	222	224	207	199	215	177	171	170
$\langle\Delta E^{H+C_T}\rangle_a$	19	12	−23	−11				
$\langle\Delta E^{H+C_T}\rangle_d$	−229	−242	−254	−255				
$\langle\Delta E^{H+C_T}\rangle_u$	248	254	229	245				
$\langle\tau_{coll}\rangle_a$	1.32	1.44	1.55	1.69	1.32	1.44	1.55	1.69
$\langle\tau_{coll}\rangle_d$	1.40	1.55	1.66	1.82	1.05	1.09	1.14	1.22
$\langle\tau_{coll}\rangle_u$	1.06	1.05	1.13	1.23	1.40	1.54	1.65	1.82

[a] E_v =40 700 cm^{-1} plus thermal energy at 300 and 600 K. The units of $\langle\Delta E\rangle$ are in cm^{-1} and the units of $\langle\tau_{coll}\rangle$ are in ps. $\langle\Delta E^{H+C_T}\rangle$ indicates the total translational energy gained or lost by the hot and cold molecules.

V−V transfer with other processes being minor channels. Comparing the first four columns that describe CET quantities in the excited molecule with the remaining four in Table 1 that describe CET quantities in the cold molecule shows that practically all of the energy lost by the hot molecule was picked up by the cold one. This does not mean that rotations and translations are not involved at all in the energy transfer process. As Table 1 shows, the up and down transitions are fairly large and can amount to 15−20% of the V−V CET transfer. The fact that their overall contribution to $\langle\Delta E_R\rangle_a$ is negligible is misleading. A graphical presentation of the results of the V/R energy transfer is provided in Figure 2, which shows the overall energy transferred, $\langle\Delta E\rangle_a$ and $\langle\Delta E_V\rangle_a$, for the hot and cold molecule in collisions of T*,pX*, and Az* with B and of B* colliding with Az. The temperature effects will be discussed later, but it is interesting that in all of these cases as well as in collisions of B* with T and pX (given in Table 2) V−V is the dominant channel with minor contributions of rotations and translations. We explain this extraordinary V−V transfer efficiency by the fact that there is a large number of low-lying gateway modes, as can be seen clearly in Appendix IV, which are very efficient in CET. The internal rotors in T and pX bath are cold and therefore are not in the way of CET, unlike the situation in hot T and pX where the rotors are excited.

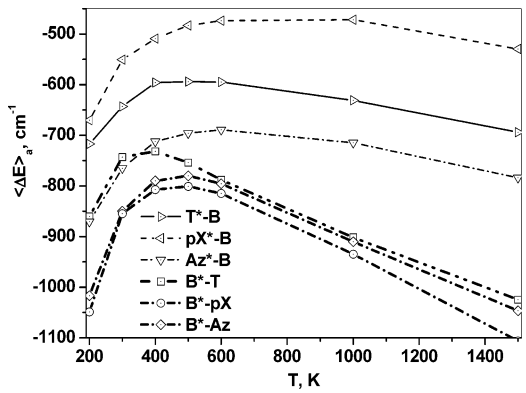

Figure 1. $\langle\Delta E\rangle_a$ vs temperature for polyatomic−polyatomic collisions. The excitation energy of the hot polyatomic molecule is 40 700 cm^{-1}. Note the high efficiency of the cold bath colliding with excited benzene.

Comparison with Experimental Results. To make the results of the calculations amenable to comparison with experiment, we use eq 3 with the actual values of σ that were used in evaluating the experimental results. Unfortunately, the experimental results of CET of the excited molecules studied here are unavailable except for B−B collisions, which were studied by Toselli and Barker[17] using IRF. They report $\langle\Delta E\rangle_d = -1477$ cm^{-1} compared to −1671 cm^{-1} found in the present work. Considering the fact that $\langle E\rangle$ in the experiment was 25 000 cm^{-1} compared to 40 700 cm^{-1} in the present work and because $\langle\Delta E\rangle$ is a function of internal energy, the agreement is acceptable. Additional comparisons with experiments are given in the discussion of the probability density function.

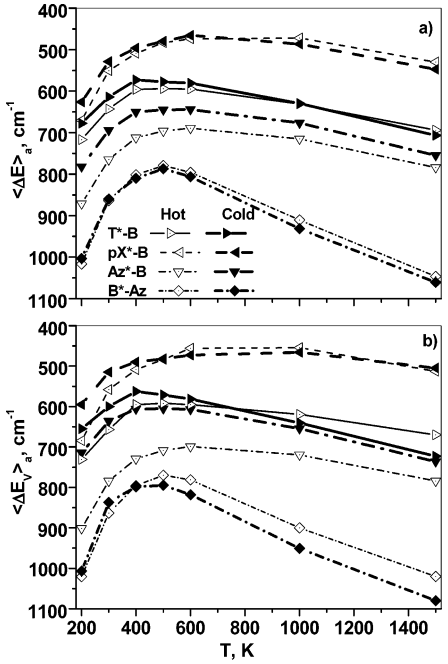

Figure 2. (a) $|\langle\Delta E\rangle_a|$ and (b) $|\langle\Delta E_V\rangle_a|$ vs temperature for polyatomic−polyatomic collisions. Energy lost by the excited molecule, empty symbols, and energy gained by the cold molecule, full symbols. The excitation energy of the hot polyatomic molecule is 40 700 cm^{-1}.

Collision Lifetime. One fact that emerges from the present calculations, and can be seen in Tables 1 and 2, is that in the hot molecule the collision duration of up collisions, $\langle\tau\rangle_u$, is much shorter than that for down collisions, $\langle\tau\rangle_d$. The fact that the values of $\langle\Delta E\rangle_d$ are much larger than $\langle\Delta E\rangle_u$ is explained by the existence of a chattering mechanism of long τ, in addition to short impulsive collisions in which energy is transferred piecemeal by multiple internal encounters of the colliding pair. This was discussed in Paper I. The values of $\langle\tau\rangle_d$, as reported in Table 1, vary a little with the mass of the excited molecule T*, pX*, and Az* colliding with B, that is, with the intermolecular potential and all colliding pairs have similar values. However, when B is excited and T, pX, and AZ are the bath, the values of $\langle\tau\rangle_d$ at low temperatures are significantly longer than the previous case because of the fact that the bath collider has unexcited low-frequency modes and unexcited internal rotors and therefore are not in the way of forming a collision complex. In up collisions, where $\langle\tau\rangle_u$ is short, the collisions are mainly impulsive.

Rotational Energy Transfer. Examination of Tables 1−3 shows that even though the overall rotational energy transfer $\langle\Delta E_R\rangle_a$, is close to zero, the up and down rotational energy transfer is fairly large and can amount to up to 20% of $\langle\Delta E\rangle_d$. Because the mechanism of CET between B*−B, Paper I, and the present P−P systems is similar, it is safe to say that the present results support the findings in Paper I that freezing the overall rotations enhances CET in a significant way. An overall view of rotational energy transfer is given in Figure 3.

Vibrational Temperatures, T_V. As indicated before, at constant excitation energy, the average energy per mode, that is, the vibrational temperature, varies with molecular size. That is to say, benzene with an excitation energy identical to that of *p*-xylene, but with a smaller number of internal modes, has a higher internal vibrational temperature. This may affect the values of the CET quantities. To check how T_V affects CET, we have calculated the CET quantities for molecules with identical vibrational temperatures, but of course, with different values of excitation energy. Table 3 shows the results of the calculations for the four molecules at ambient temperature of 300 K and T_V = 2851 K, which correspond to B excited at 40 700 cm^{-1} plus thermal energy, and the overall temperature-dependent behavior is shown in Figure 4. It is clear from the Table that the larger the molecule (and the larger the excitation energy) the higher the value of $\langle\Delta E\rangle$. However, when pX* and AZ*, which have almost identical excitation energies, are compared, AZ* is much more efficient than pX* with internal rotors. So, low-lying vibrations do help CET and internal rotations are in the way of efficient energy transfer. Therefore, when the results in Tables 1−3 are compared it is clear that T_V does affect CET but it is one parameter among few: internal rotations, collision lifetime, and translational energy being the others. The overall picture that emerges from this set of calculations supports the CET behavior discussed above.

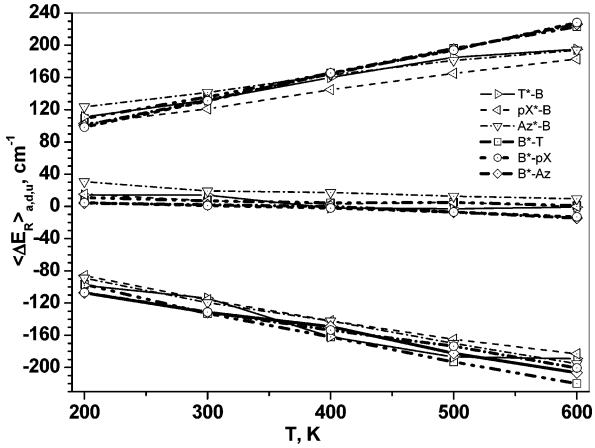

Figure 3. Average rotational energy transferred in up, down, and all collisions vs temperature. The excitation energy is 40 700 cm^{-1}. Although $\langle\Delta E_R\rangle_a$ is almost nil, the up and down values are significant.

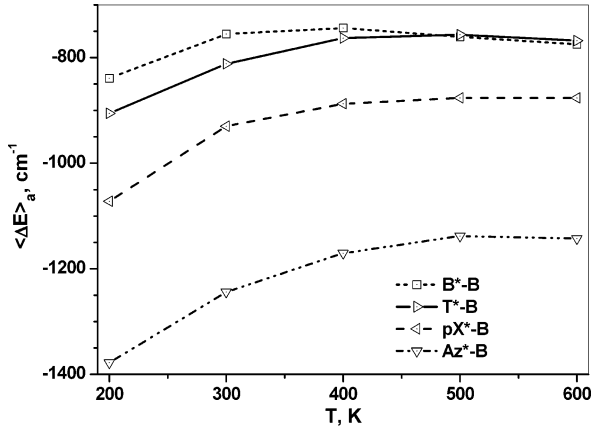

Figure 4. $\langle\Delta E\rangle_a$ vs temperature for polyatomic−polyatomic collisions. All molecules are at identical vibrational temperature at a given bath temperature. The excitation energy and vibrational temperature of each molecule are given in Appendix III.

Temperature Effects. Figure 1 shows the results for $\langle\Delta E\rangle_a$ as a function of temperature for the molecules studied. For these molecules, the absolute values of $\langle\Delta E\rangle_a$ are large at low temperatures, reach a minimum, and increase again at high temperatures. For T*, pX*, and AZ* colliding with B, the increase is very modest, whereas for B* colliding with T, pX, and AZ the increase is dramatic. An explanation for the high values of $\langle\Delta E\rangle$ at low temperatures can be found in Figure 5, which shows the values of $\langle\tau\rangle$ as a function of temperature. At

TABLE 3: Energy Transfer Quantities of Excited Benzene, Toluene, *p*-Xylene, and Azulene Colliding with Bath Benzene at 300 K[a]

	B*−B	T*−B	pX*−B	AZ*−B
E'_V, cm^{-1}	41069	53777	66597	66897
$\langle\Delta E\rangle_a$	−755	−812	−930	−1241
$\langle\Delta E\rangle_d$	−888	−959	−1093	−1413
$\langle\Delta E\rangle_u$	55	61	56	43
$\langle\Delta E_V\rangle_a$	−767	−827	−956	−1334
$\langle\Delta E_V\rangle_d$	−874	−954	−1100	−1480
$\langle\Delta E_V\rangle_u$	27	48	37	36
$\langle\Delta E_R\rangle_a$	12	15	26	92
$\langle\Delta E_R\rangle_d$	−126	−115	−112	−50
$\langle\Delta E_R\rangle_u$	144	134	142	157
$\langle\Delta E^{H+C_T}\rangle_a$	18	39	68	111
$\langle\Delta E^{H+C_T}\rangle_d$	−136	−147	−143	−142
$\langle\Delta E^{H+C_T}\rangle_u$	157	199	228	285
$\langle\tau_{coll}\rangle_a$	2.23	2.33	2.28	2.32
$\langle\tau_{coll}\rangle_d$	2.39	2.49	2.43	2.44
$\langle\tau_{coll}\rangle_u$	1.29	1.34	1.36	1.39

[a] All excited molecules have the same vibrational temperature, T_V, of 2851 K which is the T_V of benzene excited to 40 700 cm^{-1} plus the thermal energy of benzene at 300 K. The units of $\langle\Delta E\rangle$ are in cm^{-1} and the units of $\langle\tau_{coll}\rangle$ are in ps. $\langle\Delta E^{H+C_T}\rangle$ indicates the total translational energy gained or lost by the hot and cold molecules.

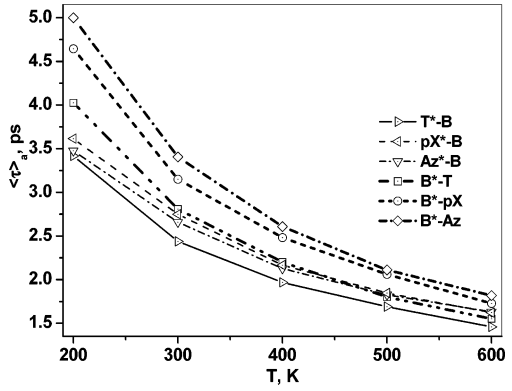

Figure 5. Average collision lifetime of all collisions vs temperature. The excitation energy is 40 700 cm^{-1}.

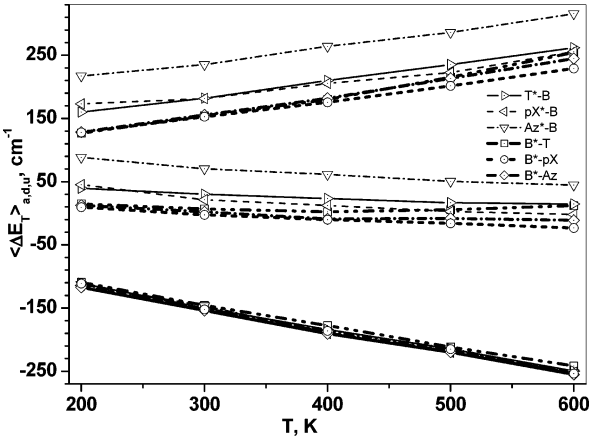

Figure 6. Average translational energy transferred in up, down, and all collisions vs temperature. The excitation energy is 40 700 cm^{-1}. Although $\langle\Delta E_T\rangle_a$ is almost nil, the up and down values are significant.

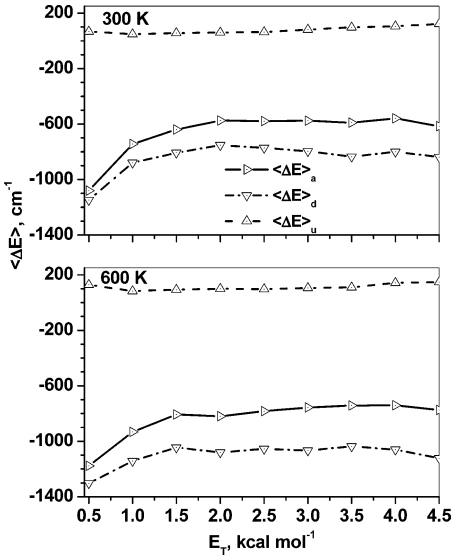

Figure 7. Average energy transferred in a bin in excited benzene−benzene collisions as a function of the initial relative translational energy at 300 and 600 K. The excitation energy is 40 700 cm^{-1}.

low temperatures, the collision complex lifetimes are long, which enable a chattering process of multiple encounters in which energy is transferred in a stepwise manner, and thus large values of $\langle\Delta E\rangle$ are obtained. Also, it is clear from Figure 5 that large bath molecules have longer collision lifetimes than smaller ones. This explains why when B*, the smallest of the lot, collides with larger bath molecules it affects large $\langle\Delta E\rangle$, whereas when the larger T*, pX*, and AZ* collide with B the collision lifetime is shorter and $\langle\Delta E\rangle$ is smaller. At high temperatures, the lifetimes of all pairs are similarly short and the collisions are impulsive. The unexcited T, pX, and AZ have low-lying gateway modes and are more efficient than B.

Translational Energy. The energy transfer process involves, in addition to V−V and V−R, also V/R−T. Tables 1 and 2 and Figure 6 show values of the average translational up, down, and all energy change in both hot and cold molecules, $\langle\Delta E_T\rangle_{u,d,a}$ as a function of the temperature. As can be seen, although the values of $\langle\Delta E_T\rangle_a$ are very small, the up and down transitions can be as much as 25% of the values of $\langle\Delta E\rangle_d$. The up collisions in the series B* colliding with T, pX, and AZ are more efficient than those in the series T*, pX*, and AZ* colliding with B. An explanation consistent with the other findings reported above is that in the first series the bath molecules have low-lying vibrations that are instrumental in the V/R/T process.

There is an effect of translational energy on the values of $\langle\tau\rangle$ and hence on the values of $\langle\Delta E\rangle$. The ΔE transferred was binned according to its initial relative translational energy and is averaged in each bin. Figure 7 shows the dependence of $\langle\Delta E\rangle$ in each bin on the initial relative translational energy at 300 and 500 K. The absolute values of $\langle\Delta E\rangle$ at low values of translational energy are high and decrease with temperature until they level off at high translational energies. Thus, at low temperatures, where the average translational energy is low and $\langle\tau\rangle$ is high, there are high values of $\langle\Delta E\rangle$. At high temperatures, however, $\langle\tau\rangle$ is lower because the average translational energy is higher and chattering does not take place and collisions are impulsive.

Probability Density Function. The probability density function, $P(E,E')$, which is used in master equation calculations and plays a major role in the interpretations of experimental results, is an elusive commodity that was not found, yet, experimentally or from basic principles. During the past few years, many models for CET were developed,[1] but they lack first-principle foundations. Trajectory calculations come close to the

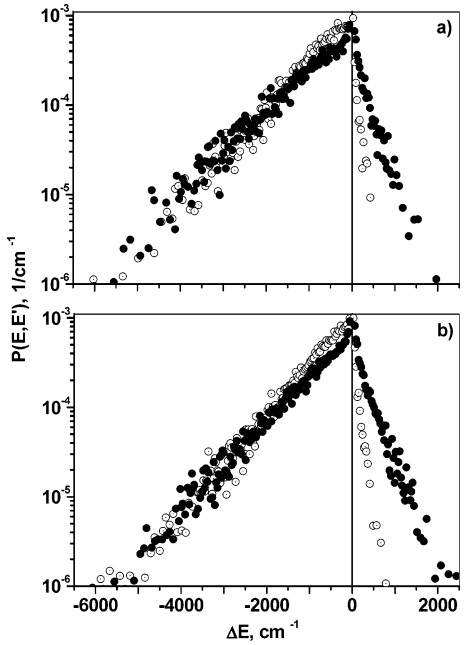

Figure 8. $P(E,E')$ of (a) excited toluene and (b) excited *p*-xylene in collisions with benzene at 200 K (empty symbols) and 600 K (full symbols) vs ΔE. The excitation energy is 40 700 cm^{-1}. There is a noticeable supercollision tail at high energies at the down-collision part.

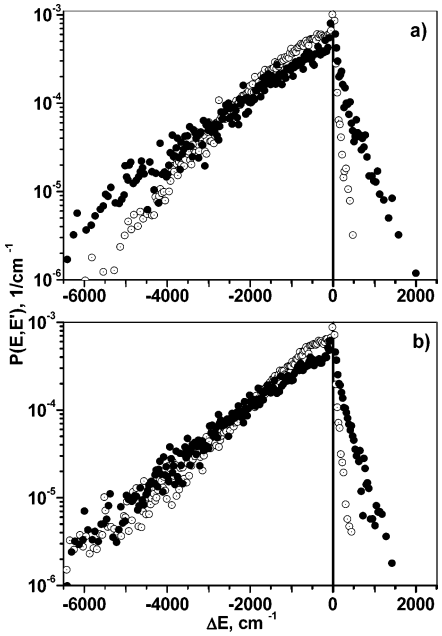

Figure 9. $P(E,E')$ of (a) excited azulene in collisions with benzene and (b) excited benzene in collision with toluene at 200 K (empty symbols) and 600 K (full symbols) vs ΔE. The excitation energy is 40 700 cm^{-1}. There is a noticeable supercollision tail at high energies at the down-collision part.

first-principles method, but they also have their shortcomings; the major one being the uncertainty in the value of the 0−0 peak. Therefore, we report the data of $P(E,E')$ for various excited and bath molecules at various initial conditions but will not give fitting parameters, which depend on the value of the 0−0 peak.

Figures 8 and 9 show $P(E,E')$ for collisions of T*, pX*, and AZ* with B and collisions of B* with T all at 200 K and at 600 K. One feature that emerges very clearly from the figures is that there is a supercollision tail at all temperatures for all collision pairs. This is no new fact and augments studies

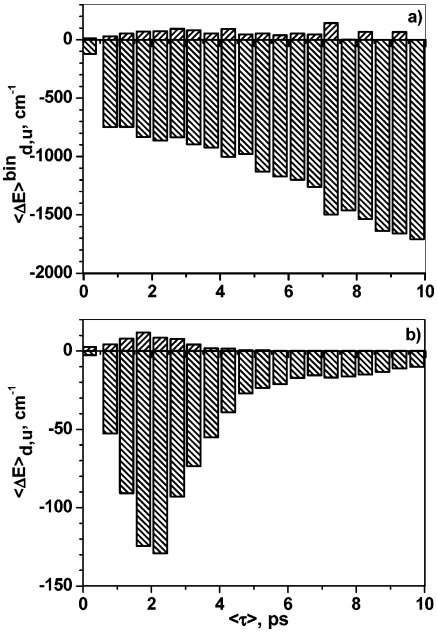

Figure 10. Average energy transferred in a given lifetime for excited azulene colliding with benzene at 200 K. (a) as a function of collision lifetime. (b) The data in a is weighted by the probability of obtaining a given value of τ. It is clear from a that the longer the collision complex lives the more energy is transferred, and it is clear from b that there is a long tail at high values of τ during which chattering collisions occur.

performed previously on the subject.[3,5] Another feature that is common in all figures is the fact that the low-temperature data on the down collision side form convex lines. Actually, some $P(E,E')$ have a distinct peak on the down collision side away from the 0−0 peak. The high-temperature data, however, can be represented by concave lines. If one was to fit the points to the stretched exponential function of Lenzer, Luther, and coworkers[18]

$$P(E,E') = \alpha \exp(-\Delta E/\alpha)^Y \qquad (4)$$

where α and Y are fitting parameters, then at 200 K $Y < 1$, which indicates a convex lines, and at 600 K $Y > 1$, which indicates concave lines. Thus, the shape of the $P(E,E')$ is temperature-dependent. This conclusion augments the findings in Paper I on B*−B collisions and in Higgins and Chapman's work on the pyrazine−CO system[19] discussed in paper I. A possible explanation for the off 0−0 peak at low temperatures is that because $\langle\tau\rangle$ is long at low temperatures the chattering mechanism is operative and $\langle\Delta E\rangle$ is large as indeed is seen in Tables 1−3 and Figures 1 and 2. Therefore, at low temperatures there is a maximum in $P(E,E')$, which leads to large absolute values of $\langle\Delta E\rangle$. Added support for this explanation can be found in Figures 10 and 11 where the average energy transferred in a given lifetime is shown as a function of collision lifetime for two temperatures. Figure 10 shows excited AZ colliding with B at 200 K. From part a it is clear that the longer the collision complex lives the more energy is transferred. Part b shows that when the data in a is weighted by the probability of obtaining a given value of τ, the average $\langle\tau\rangle$ is long and there is a long tail at high values of τ during which chattering collisions occur. Figure 11 shows the same data at 600 K. Here the situation is totally different, $\langle\tau\rangle$ is short, and there is no significant tail at longer times. That is to say, very little chattering collisions and less energy is transferred.

Polyatomic−Ar Collisions. An extensive discussion of polyatomic−monatomic, PM, CET was presented in paper I and a

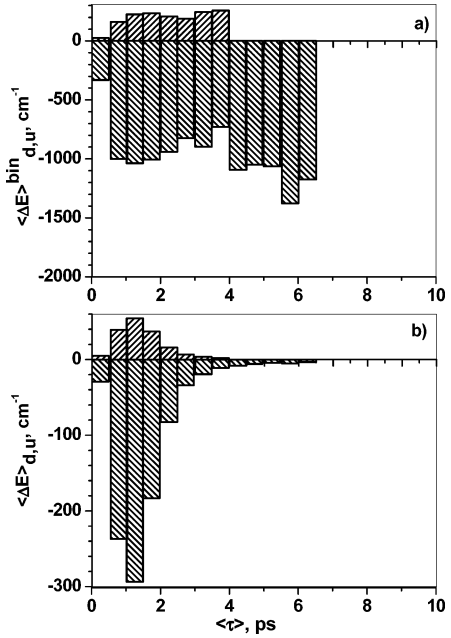

Figure 11. Average energy transferred in a given lifetime for excited azulene colliding with benzene at 600 K (a) as a function of collision lifetime. (b) The data in a is weighted by the probability of obtaining a given value of τ. It is clear from b that there is no long tail at high values of τ during which chattering collisions can occur.

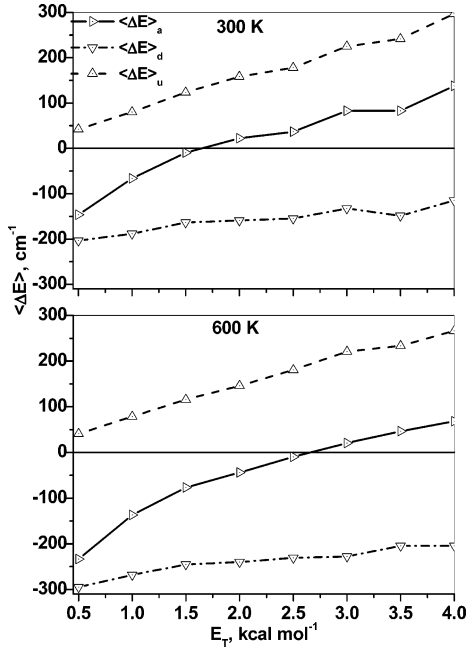

Figure 12. Average energy transferred in a bin in excited benzene−Ar collision as a function of the initial relative translational energy at 300 and 600 K. The excitation energy is 40 700 cm^{-1}.

comparison was made to PP CET. These conclusions were based on B*−B and B*−Ar collisions and are listed in the Introduction. Here we expend our study of PM collisions to include T*, pX*, and AZ* collisions with Ar. Table 4 shows the results of CET parameters at 300 and 600 K.[20] The values of $\langle\Delta E\rangle_a$ do not differ significantly from one another, so the overall conclusion is that internal rotations do not inhibit V−T energy transfer in PM. If at all, they enhance up and down vibrational energy loss and gain, $\langle\Delta E_V\rangle_{u,d}$. Despite the diversity of structures, the balance of gain and loss leads to only small differences in the values of $\langle\Delta E\rangle_a$. Here again, $\langle\Delta E\rangle_a$ in AZ*−Ar collisions is the largest because of the many low-frequency gateway modes in AZ. Similar results were obtained in trajectory calculations by Linhanata and Lim[21,22] on CET in ethane and propane, which show that the effect of free rotors on $\langle\Delta E\rangle_a$ is very small. Another feature of PM collisions is the short collision lifetime. This supports our previous finding that CET in PM is impulsive. In addition, we found that impulsive collisions cause overall rotations to play a major role in the mechanism of energy transfer. This in contrast to PP collisions where many collisions form long-lived complexes and energy is transferred by multiple encounters, chattering.

Another difference between PP and PM CET that emerges from the present study is the dependence of ΔE on the translational energy. Figure 12 shows the average energy transferred in a B−Ar collision in a given initial translational energy at 300 K and at 600 K. The lines at the two temperatures are similar and differ from each other only in details because the overall rotations are a function of temperature and affect the mechanism of energy transfer. The figure shows that the vibrational−rotational energy transfer depends almost linearly on the translational energy. This is in contrast to the B*−B collisions depicted in Figure 7 where the average energy transferred reaches a plateau at higher translational energies.

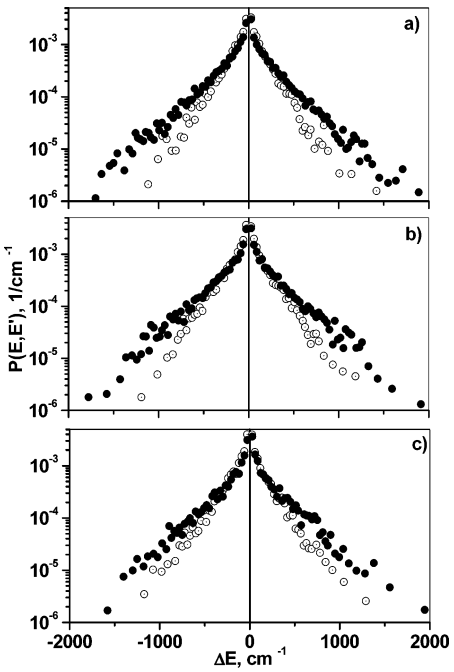

Figure 13. $P(E,E')$ of (a) benzene, (b) toluene, and (c) *p*-xylene in collisions with Ar at 300 K (○) and 600 K (●) and $\epsilon/\Delta t = 0.35$ cm^{-1}/fs. The excitation energy is 40 700 cm^{-1}. The lines become progressively more concave and there is a noticeable supercollision tail at high energies at the down-collision part.

The data in Figure 12 supports the mechanism of short, impulsive collisions for PM in contrasted to PP collisions, which, in addition to impulsive collisions, have a large fraction of long-lived chattering collisions. Figure 13 shows $P(E,E')$ for B*, T*, and pX* colliding with Ar at 300 and 600 K. The lines are concave and become more so as the temperature increases. For all of the lines, Y in eq 4 is <1.0. This is in contrast to the shape of $P(E,E')$ of PP collisions, which is convex at low temperatures and becomes concave only at high temperatures.

TABLE 4: Energy Transfer Quantities of the Excited Molecule in Polyatomic−Ar Collisions at Various Temperatures[a]

	B*−Ar	T*−Ar	pX*−Ar	AZ*−Ar	B*−Ar	T*−Ar	pX*−Ar	AZ*−Ar
		$T = 300$ K				$T = 600$ K		
$\langle\Delta E\rangle_a$	−7	−12	−15	−41	−13	−8	1	−47
$\langle\Delta E\rangle_d$	−112	−130	−127	−170	−197	−203	−194	−268
$\langle\Delta E\rangle_u$	104	115	114	109	170	199	194	194
$\langle\Delta E_V\rangle_a$	−15	−14	−10	−47	−25	−5	6	−43
$\langle\Delta E_V\rangle_d$	−81	−103	−102	−159	−137	−156	−146	−242
$\langle\Delta E_V\rangle_u$	61	85	87	93	101	150	145	175
$\langle\Delta E_R\rangle_a$	7	2	−5	7	13	−4	−5	−4
$\langle\Delta E_R\rangle_d$	−98	−93	−93	−96	−165	−156	−144	−172
$\langle\Delta E_R\rangle_u$	108	97	97	103	183	154	138	168
$\langle\Delta E^{H+C_T}\rangle_a$	−2	−5	−7	−22	−4	−3	1	−25
$\langle\Delta E^{H+C_T}\rangle_d$	−36	−51	−58	−89	−64	−81	−88	−141
$\langle\Delta E^{H+C_T}\rangle_u$	33	45	50	57	54	78	87	102
$\langle\tau_{coll}\rangle_a$	1.41	1.37	1.34	1.46	0.88	0.84	0.88	0.95
$\langle\tau_{coll}\rangle_d$	1.41	1.39	1.38	1.44	0.90	0.83	0.87	0.94
$\langle\tau_{coll}\rangle_u$	1.41	1.35	1.30	1.48	0.86	0.85	0.89	0.95

[a] E_v =40 700 cm^{-1} + thermal energy. The units of $\langle\Delta E\rangle$ are in cm^{-1} and the units of $\langle\tau_{coll}\rangle$ are in ps. $\langle\Delta E^{H+C_T}\rangle$ indicates the total translational energy gained or lost by the hot and cold molecules.

Summary. Collisions between excited toluene, *p*-xylene, and azulene with benzene bath and collisions of excited benzene with toluene, *p*-xylene, and azulene bath at various temperatures shed light on the mechanism of energy transfer between large aromatic molecules. These results, together with those presented in Paper I, pinpoint the major mechanistic features of the energy transfer process in large aromatic molecules. A comparison is made with collisional energy transfer between excited polyatomic aromatic molecules and a monatomic bath, Ar in the present case. The major findings for aromatic polyatomic-polyatomic collisions are: (a) Energy transfer takes place mainly via V−V energy transfer with V−R and V/R−T contributions. (b) Up and down rotational energy exchange takes place during collisions, but the overall average rotational energy exchange is very small. (c) Internal rotations in the excited molecule hinder energy exchange, whereas in the bath molecule they do not because the internal rotors are not excited. (d) Energy transfer at low and high temperatures is more efficient than that at intermediate temperatures. (e) Low-frequency modes enhance energy transfer. Thus, azulene with the same number of normal modes as *p*-xylene but with modes of lower frequencies and without internal rotations is much more efficient in transferring energy to benzene bath molecules. (f) Energy transfer depends on the initial relative translational energy at lower values and reaches a plateau at higher values. (g) Vibrational temperatures affect energy transfer. In a series of polyatomic molecules of different sizes and identical vibrational temperature, that is, different excitation energies, the largest values of $\langle\Delta E\rangle_a$ occur in the largest molecules with the lowest frequency modes. (h) Collisional energy transfer probability density function, $P(E,E')$, in aromatic polyatomic−polyatomic collisions is convex at low temperatures and can be concave at high temperatures. (i) There is a clear supercollision tail at the down wing of $P(E,E')$. (j) A mechanism for obtaining high values of $\langle\Delta E\rangle$, in addition to short impulsive collisions, is chattering collisions where energy is transferred in a sequence of short encounters during the lifetime of the collision complex. (k) The collision lifetime is long, >2ps, at low temperatures. This enables many chattering collisions to take place, and therefore this is one of the main reasons for the large values of $\langle\Delta E\rangle_a$.

To summarize, the mechanism of collisional energy transfer in aromatic polyatomic−polyatomic collisions is via short, impulsive collisions and long chattering collisions, which are operational at low temperatures.

Comparison of aromatic polyatomic−polyatomic collisions with polyatomic−Ar collisions shows that there are mechanistic similarities: (a) In both cases, rotations and translations play a role in the energy transfer process but the average total rotational energy exchanged is small. (b) Low-frequency modes are gateway modes. However, there are differences as well: (a) In polyatomic−monatomic collisions, internal rotations do not inhibit energy transfer as is the case in polyatomic−polyatomic collisions. (b) The values of $\langle\Delta E\rangle_u$ and $\langle\Delta E\rangle_d$ in polyatomic−monatomic collisions are affected by the temperature. However, the overall energy transfer, $\langle\Delta E\rangle_a$, which is the sum of the two, is not. (c) Unlike in aromatic polyatomic−polyatomic collisions, energy transfer in polyatomic−monatomic collisions is linearly dependent on initial relative translational energy. (d) The collisional energy transfer probability density function, $P(E,E')$, in polyatomic−monatomic collisions is concave at all temperatures, whereas in polyatomic−polyatomic collisions it is convex at low temperatures.

Acknowledgment. This work is supported by the Technion V. P. R. Fund, by the E. and M. Mendelson Research Fund, by the fund for promotion of research at the Technion, and by the Ministry of Science and the Arts under the KAMEA program.

Appendix I

TABLE 5: Lennard−Jones Parameters for Polyatomic−Polyatomic Collisions

	σ_{LJ} (nm) [a]	ϵ_{LJ}/k (K) [a]	refs	σ (nm) [b]	ϵ_{LJ}/k (K) [b]
benzene	0.546	401	23	0.546	395
toluene	0.592	410	24	0.584	447
p-xylene	0.621	438	25	0.620	494
azulene	0.661	523	26	0.655	605
benzene toluene	0.569	406	[c]	0.565	420
benzene *p*-xylene	0.584	419	[c]	0.583	442
benzene azulene	0.604	458	[c]	0.601	489

[a] Experimental values. [b] Calculated values by program SIGMON[12] from pairwise LJ parameters used in this work. $\sigma_{HH} = 0.282$ nm, $\sigma_{CH} = 0.297$ nm, $\sigma_{CC} = 0.312$ nm; $\epsilon_{HH}/k = 8.04$ K, $\epsilon_{CH}/k = 14.23$ K, $\epsilon_{CC}/k = 25.18$ nm. [c] Parameters σ_{LJ} and ϵ_{LJ}/k were calculated from the appropriate combination rules.[10] Note: The value of σ for *p*-xylene reported in refs 24, 27, and 28 is smaller than that of benzene and toluene, a highly unreasonable situation, and is in error. The value reported by Vogel and Hendl[25] is very reasonable. The values of σ that are reported by them for benzene and toluene, 0.538 and 0.588 nm, respectively, agree well with accepted literature values. This lends credit to their vapor-phase viscosity measurements including the *p*-xylene value.

Appendix II

TABLE 6: LJ Pairwise Parameters for Polyatomic−Ar Collisions and Effective Overall σ and ϵ

	benzene−Ar		toluene−Ar		*p*-xylene−Ar		azulene−Ar	
	H−Ar	C−Ar	H−Ar	C−Ar	H−Ar	C−Ar	H−Ar	C−Ar
σ_{ij} (nm)	0.318	0.333	0.340	0.356	0.334	0.350	0.323	0.337
ϵ_{ij}/k (K)	28.62	50.64	23.67	41.88	22.04	38.99	27.59	48.81
	calcd[a]	ref[b]	calcd	ref	calcd	ref	calcd	ref
σ_{P-Ar} (nm)	0.447	0.447	0.477	0.470	0.483	0.484	0.504	0.504
ϵ_{P-Ar}/k (K)	213	214	216	216	224	224	244	244

[a] Calculated values from pairwise LJ parameters used in this work. [b] Obtained from the combination rules: $\sigma_{P-Ar} = 0.5(\sigma_{P+}\sigma_{Ar})$, $\epsilon_{P-Ar} = (\epsilon_{p*}\epsilon_{Ar})^{0.5}$, P indicates a polyatomic molecule. The values for σ_p and ϵ_P were taken from appendix I. The values for Ar are $\sigma_{Ar} = 0.347$ nm, $\epsilon_{Ar}/k = 114$ K. Note: The LJ pairwise parameters for toluene−Ar used in previous work by us[7] and by others[11] are erroneous. All of the data for toluene−Ar were recalculated. [c] The BSSH pairwise intermolecular potential[13,29] is given by: $V_{ij} = A_{ij}/r_{ij}^{\alpha} - B_{ij}(1/r_{ij}^{6} - C_{ij}/r_{ij}^{7})$; $i,j = 1-6$; and the parameters for the BSSH intermolecular potential for the benzene/Ar system are: $\alpha = 13.305$, $A_{H-Ar} = 77.211 \times 10^{-7.305}$ cm^{-1} nm$^{13.305}$; $B_{H-Ar} = 120.279 \times 10^{-3}$ cm^{-1} nm^{6}; $C_{H-Ar} = 0.27149$ nm; $A_{C-Ar} = 287.901 \times 10^{-6.305}$ cm^{-1} nm$^{13.305}$; $B_{C-Ar} = 343.979 \times 10^{-3}$ cm^{-1} nm^{6}; $C_{C-Ar} = 0$ nm.

Appendix III

TABLE 7: Vibrational Excitation Energies, E_V, at Vibrational Temperatures, T_V of Excited Benzene at Various Ambient Temperatures. Benzene Excitation Energy Is 40 700 cm^{-1}

		E_V, kcal mol^{-1}			
T, K	T_V, K	benzene	toluene	*p*-xylene	azulene
200	2837	116.6	152.7	189.2	190.0
300	2851	117.4	153.8	190.4	191.3
400	2879	118.9	155.8	192.9	193.8
500	2917	121.1	158.6	196.3	197.2
600	2965	123.8	162.1	200.7	201.6

Appendix IV

TABLE 8: Experimental and Calculated Normal Mode Frequencies

benzene									
calculated									
E_{2u}	E_{2g}	B_{2g}	A_{2u}	E_{1g}	A_{1g}	E_{1u}	E_{2u}	B_{1u}	B_{2g}
400	617	657	680	833	926	991	1015	1026	1070
E_{2g}	B_{2u}	A_{2g}	E_{1u}	E_{2g}	B_{2u}	E_{1u}	A_{1g}	E_{2g}	B_{1u}
1134	1173	1375	1531	1739	1749	3057	3057	3059	3060
experimental[a,b]									
398	606	707	673	846	993	1037	967	1010	990
1178	1146	1350	1482	1600	1309	3068	3073	3056	3057
toluene									
calculated									
A_2	B_2	B_1	A_2	B_2	A_1	B_1	B_2	A_1	B_2
1	214	329	385	479	496	616	645	766	869
A_1	A_2	B_1	A_1	B_2	B_1	B_2	A_1	B_1	A_2
957	960	976	1007	1018	1047	1122	1129	1160	1170
A_1	B_2	B_1	B_1	B_2	A_1	B_1	A_1	B_1	B_1
1216	1246	1338	1479	1483	1494	1499	1586	1727	1749
A_1	A_1	B_2	B_1	A_1	B_1	A_1	B_1	A_1	
1777	2859	2974	2975	3057	3057	3058	3059	3060	
experimental[c]									
	217	344	408	464	521	623	695	784	728
1003	843	1040	1030	893	1080	978	1175	1154	964
1208	140	1312	1460	1460	1379	1460	1494	1494	1586
1605	2921	2979	2952	3055	3029	3063	3039	3087	

TABLE 8 (Continued)

p-xylene									
calculated									
A_u	B_{1g}	B_{3u}	B_{2u}	B_{2g}	B_{3g}	A_u	A_g	B_{3u}	B_{3g}
1	2	140	272	323	383	385	431	536	616
B_{2g}	B_{1u}	B_{3u}	A_g	B_{1g}	B_{2g}	A_u	B_{2u}	B_{2g}	B_{1u}
665	669	806	955	960	973	993	1005	1030	1089
B_{3u}	B_{2g}	B_{2u}	A_g	B_{1u}	A_g	B_{3g}	B_{2u}	B_{1u}	A_g
1100	1113	1170	1195	1217	1234	1317	1443	1483	1483
B_{2u}	B_{3g}	B_{3u}	B_{2g}	B_{2u}	B_{1u}	B_{3g}	A_g	B_{2u}	A_g
1483	1486	1487	1517	1640	1716	1746	1801	2859	2859
B_{1u}	B_{3g}	B_{3u}	B_{3g}	B_{3g}	B_{1u}	B_{2u}	A_g		
2974	2974	2975	2975	3057	3058	3059	3059		
experimental[d]									
15	15	132	285	312	389	410	454	481	643
700	694	795	830	832	930	972	972	972	1026
1032	1032	1099	1183	1225	1203	1313	1320	1385	1378
1400	1416	1458	1446	1458	1520	1579	1616	2950	2950
2950	2950	2950	2950	3050	3050	3050	3050		
azulene									
calculated									
A_2	B_2	B_1	B_2	A_1	B_1	A_2	B_2	B_2	A_1
174	174	326	335	373	404	405	456	596	600
B_1	A_2	A_1	A_1	B_2	B_2	A_1	A_2	B_1	A_2
666	731	753	806	873	913	975	982	1069	1072
B_2	A_1	B_2	A_1	B_1	B_1	A_2	B_1	B_2	B_1
1117	1148	1178	1193	1198	1223	1252	1283	1322	1327
A_1	B_1	A_1	B_1	A_1	A_1	B_1	B_1	A_1	B_1
1357	1480	1569	1634	1714	1786	1806	1920	1991	2036
A_1	A_1	A_1	B_1	A_1	B_1	B_1	A_1		
3032	3033	3033	3033	3034	3034	3039	3043		
experimental[e]									
189	240	323	304	406	486	331			680
987	542	825	900	762	795	1210	813	1012	911
952	971	965	1160	712	1049	941	1117	1085	1216
1268	1160	1396	1378	1448	1457	1443	1480	1579	1536
2968	3037	3037	3018	3072	3042	3098	3077		

[a] Eaton, V. J.; Steele, D. *J. Mol. Spectrosc.* **1973**, *48*, 446. [b] Pearce, R. A. R.; Steele, D.; Radcliffe, K. *J. Mol. Struct.* **1973**, *15*, 409. [c] Fuson, N.; Garrigou-Lagrange, C.; Josien, M.L. *Spectrochim. Acta* **1960**, *16*, 106. [d] Draeger, J. D. *Spectrochim. Acta* **1985**, *41A*, 607. [e] Varsanyi, G. A*ssignments for Vibrational Spectra of Seven Hundred Benzene Derivatives*; Wiley: New York, **1974**; Vol. 1. [f] Chao, R. S.; Khanna, R. K. S*pectrochim*. Acta, **1977**, *33A*, 39.

References and Notes

(1) Oref, I.; Tardy, D. C. *Chem. Rev.* **1990**, *90*, 1407.
(2) Lenzer, T.; Luther, K. *Phys. Chem. Chem. Phys.* **2004**, 6, 955.
(3) Bernshtein, V.; Oref, I. *J. Phys. Chem. B* **2005**, *109*, 8310.
(4) Clary, D. C.; Gilbert, R. G.; Bernshtein, V.; Oref, I. *Faraday Discuss*. **1995**, *102*, 423.
(5) Bernshtein, V.; Oref, I. *J. Chem. Phys.* **1997**, *106*, 7080.
(6) Oref, I. Supercollisions. In *Energy Transfer from Large Molecules in Nonreactive Systems, Advances in Chemical Kinetics and Dynamics Series*; Barker, J. R., Ed.; JAI Press: London, 1995; Vol. 2B, pp 285−298.
(7) Bernshtein, V.; Lim, K. F.; Oref, I. *J. Phys. Chem*. **1995**, *99*, 4531.
(8) Bernshtein, V.; Oref, I. *Chem. Phys. Lett*. **1995**, *233*, 173.
(9) Draeger, J. A. *Spectrochim. Acta* **1985**, *41A*, 607.
(10) Lim, K. F.; Gilbert, R. G. *J. Phys. Chem*. **1990**, *94*, 77.
(11) Lim, K. F. *J. Chem. Phys*. **1994**, *100*, 7385.
(12) Lim, K. F. Program *SIGMON*: *An Aid for the Semiempirical Fitting of the Intermolecular Potential*; School of Biological and Chemical Sciences, Deakin University, Geelong, VIC 3217, Australia, 1992.
(13) Bludsky, O.; Spirko, V.; Hrouda, V.; Hobza, P. *Chem. Phys. Lett*. **1992**, *196*, 410.
(14) Hase, W. L.; Duchovic, R. J.; Hu, X.; Komornicki, A.; Lim, K. F.; Lu, D.-H.; Peslherbe, G. H.; Swamy, K. N.; Vande-Linde, S. R.; Varandas, A.; Wang, H.; Rolf, R. J. Venus: Quantum Chemistry Program. *Exch. Bull.* **1996**, *16*, 43; QCPE Program 671.
(15) Nakashima, N.; Yoshihara, K. *J. Chem. Phys.* **1983**, *79*, 2727.
(16) Bernshtein, V.; Oref, I. *J. Phys. Chem. A.* **2000,** *104*, 706.
(17) Toselli, B. M.; Barker, J. R. *J. Chem. Phys.* **1992**, *97*, 1809.
(18) Lenzer, T.; Luther, K.; Reihs, K.; Symonds, A. C. *J. Chem. Phys.* **2000**, *112*, 4090.
(19) Higgins, C. J.; Chapman, S. *J. Phys. Chem. A.* **2004**, *108*, 8009.
(20) Previous results of T*−Ar collisions by various groups, including us, were based on wrong pairwise Lennard−Jones parameters. The parameters given in the Appendix are the corrected ones.
(21) Linhantana, A.; Lim, K. F. *Phys. Chem. Chem. Phys.* **1999**, *1*, 3467.
(22) Linhantana, A.; Lim, K. F. *Phys. Chem. Chem. Phys.* **2000**, *2*, 13851.
(23) Hippler, H.; Troe, J.; Wendelken, H. J. *J. Chem. Phys.* **1983**, *78*, 6709.
(24) Mourits, F. M.; Rummens, F. H. A. *Can. J. Chem*. **1977**, *55*, 3007.
(25) Vogel, E.; Hendl, S. *Fluid Phase Equilib.* **1992**, *79*, 313.
(26) Hippler, H.; Lindemann, L.; Troe, J. *J. Chem. Phys.* **1985**, *83*, 3906.
(27) Nasehzadeh, A.; Mohseni, M.; Azizi, K. *J. Mol. Struct.: THEOCHEM* **2002**, *589*, 329.
(28) Goldman, S. *J. Phys. Chem.* **1975**, *80*, 1697.
(29) Vacek, J.; Hobza, P.; Jortner, J. *J. Phys. Chem. A* **1998**, *102*, 8268.